XLIII CILAMCE
21–25, November, 2022
FOZ DO IGUAÇU – PR – BRAZIL

Modeling and Numerical Simulation of Drug Transport and Absorption in a Tumor

Daniela Cortes[1], Giuseppe Romanazzi[1]

[1]*Dept. of Mathematics, State University of Campinas.*
Rua Sérgio Buarque de Holanda 651, 13083-859, SP/Campinas, Brasil
danielac@ime.unicamp.br, *groman@unicamp.br*

Abstract. This work describes the diffusion-convection process of transport of the drug (doxorubicin) administered by bolus injection through the tumor and interstitium. We numerically solve a coupled system of partial differential equations that models the drug transport, its uptake, and effect in the tumor.

It is used a high order finite difference method that allows to accurately describe the drug effect in the tumor. In fact, we can determine the time needed by the drug to reduce the tumor cell density and approximate the drug spatial distribution in the tumor and interstitium. In addition, the simulations shows how the doxorubicin effect in the tumor increases as its dose level increases.

Keywords: Drug Transport and Diffusion, Drug Uptake in Tumor Cells, Finite Difference Method.

1 Introduction

Anticancer drug transport and uptake in tumors have been extensively studied, see Baxter and Jain [1], Eikenberry [2], Liu et al. [3], Zhan et al. [4]. El-Kareh and Secomb [5] and Eikenberry [2]. These models do not consider the influence of blood and lymphatic vessels or realistic tumor geometry. Zhan et al. [4], on the other hand, consider these effects but not account cell proliferation and physiological degradation on the rate of change in tumor cell density. In this work, we consider instead all these factors in the tumor cell density and drug transport mathematical model and describe their effects on drug distribution and mass tumor reduction.

The partial differential equations model used are described in section 2. In section 3, we present the discrete operators and the numerical discretization of the model similar to that presented in Borges et al. [6]. In section 4, numerical experiments illustrating the behavior of the mathematical model are included. Finally, in section 5, we present some conclusions.

2 Formulation of problem

We assume the following simplifications in our model. The geometry of the tumor is spherical, with a radius of R_o, the tumor's interior is located in the center and occupies the volume of a sphere of radius R_i. Doxorubicin concentrations and tumor density depend on time and on the distance r respect the sphere center. The model has two boundaries: an internal between the tumor and normal tissue and the outer of the normal tissue. On the interior boundary, conditions of continuity for the free concentration and fluid flux are applied and, on the outer border, zero flux of drug concentration is assumed, the velocity and diffusion coefficient are supposed constant in time and space.

Free doxorubicin transport in the tumor under the above assumptions is described by the following partial differential equation with initial and boundary conditions

$$\begin{cases} \frac{\partial C_f}{\partial t}(r,t) + \frac{1}{r^2}\frac{\partial}{\partial r}\left(r^2 C_f(r,t)v(r,t)\right) = D_f \frac{1}{r^2}\frac{\partial}{\partial r}\left(r^2 \frac{\partial C_f}{\partial r}(r,t)\right) + S_i, \quad t \in [0,T), \quad r \in (0,R_o), \\ v(r,t)C_f(r,t)\Big|_{r=R_o} - D_{fn}\frac{\partial C_f}{\partial r}(r,t)\Big|_{r=R_o} = 0, \\ v(r,t)C_f(r,t)\Big|_{r=R_i^-} - D_{ft}\frac{\partial C_f}{\partial r}(r,t)\Big|_{r=R_i^-} = v(r,t)C_f(r,t)\Big|_{r=R_i^+} - D_{fn}\frac{\partial C_f}{\partial r}(r,t)\Big|_{r=R_i^+}, \\ C_f(r,t)\Big|_{r=R_i^-} = C_f(r,t)\Big|_{r=R_i^+}, \quad \frac{\partial C_f}{\partial r}(r,t)\Big|_{r=0} = 0, \\ C_f(r,0) = 0, \forall r \in (0,R_o). \end{cases} \tag{1}$$

where C_f is the free doxorubicin concentration, $r = 0$ represents the tumor center, v is the velocity of the interstitial fluid, D_f is the corresponding diffusion coefficient that is, D_{ft} in the tumor and D_{fn} in the normal tissue. S_i is the net rate of doxorubicin gained from the surrounding environment given by $S_i = S_v + S_b + S_u$, in which S_v is the net doxorubicin gained from the blood/lymphatic vessels given by the difference of doxorubicin gained from the normal tissues $F_s(t, C_v, C_f)$ and by the doxorubicin loss to the lymphatic vessels per unit volume of tissue $F_{ls}(C_f)$. That is, $S_v = F_s - F_{ls}$.

On the other hand, S_b represents the association /dissociation with bound doxorubicin-protein

$$S_b = k_d C_b(r,t) - k_a C_f(r,t), \tag{2}$$

where k_a and k_d are the doxorubicin-protein binding and dissociation rate, respectively. Finally, S_u represents the influx/efflux from tumor cells

$$S_u = V_{max}\left(\frac{C_i(r,t)}{C_i(r,t)+k_i} - \frac{C_f(r,t)}{C_f(r,t)+k_e\varphi}\right)D_c(r,t), \tag{3}$$

where D_c is the tumor cell density, k_e and k_i are parameters obtained from experimental data, V_{max} is the rate of trans-membrane transport and φ is the volume fraction of extracellular space.

Remark 1: Note that $S_i = S_v + S_b$ in the interstitium surrounding the tumor (R_i, R_o) and in the tumor $(0, R_i)$ we have $S_i = S_u$.

In (R_i, R_o), some proteins can bind to the free drug C_f, and transform into bound doxorubicin C_b, as it is described in the following C_b equation with its boundary and initial conditions

$$\begin{cases} \frac{\partial C_b}{\partial t}(r,t) + \frac{1}{r^2}\frac{\partial}{\partial r}\left(r^2 C_b(r,t)v(r,t)\right) = D_b \frac{1}{r^2}\frac{\partial}{\partial r}\left(r^2 \frac{\partial C_b}{\partial r}(r,t)\right) + k_a C_f(r,t) - k_d C_b(r,t), \quad t \in [0,T), \\ v(r,t)C_b(r,t)\Big|_{r=R_o} - D_b\frac{\partial C_b}{\partial r}(r,t)\Big|_{r=R_o} = 0, \\ v(r,t)C_b(r,t)\Big|_{r=R_i} - D_b\frac{\partial C_b}{\partial r}(r,t)\Big|_{r=R_i} = 0, \\ C_b(r,0) = 0, \forall r \in (R_i, R_o). \end{cases} \tag{4}$$

where the parameters k_a and k_d are given in eq. (2).

Along the time, an amount of free doxorubicin crosses the border of the tumor into its interior. This doxorubicin is called intracellular, denoted by C_i satisfies the following ordinary differential equation

$$\begin{cases} \frac{\partial C_i}{\partial t}(r,t) = V_{max}\left(\frac{C_f(r,t)}{C_f(r,t)+k_e\varphi} - \frac{C_i(r,t)}{C_i(r,t)+k_i}\right), \\ C_i(r_i,0) = 0. \end{cases} \tag{5}$$

Finally, we have the relationship between intracellular concentration and cell density D_c

$$\begin{cases} \frac{\partial D_c}{\partial t}(r,t) = \left(k_p - \frac{f_{max}C_i(r,t)}{C_i(r,t)+EC_{50}}\right) D_c(r,t) - k_m D_c^2(r,t), \\ D_c(r_i,0) = D_{c_0}. \end{cases} \tag{6}$$

The term f_{max} is the cell-kill rate constant and EC_{50} is the drug concentration producing 50% of f_{max}. k_p and k_m are the cell proliferation rate constant and physiologic degradation rate, respectively.

Remark 2: All the parameters described in the previous equations are taken from Zhan et al. [4] and El-Kareh and Secomb [5].

3 Numerical Discretization and Discrete Operators

In this section we describe the numerical method used to approximate the solution of eq. (1), eq. (4), eq. (5) and eq. (6) and its finite difference operators. First, we introduce the spatial domain $[0, R_o]$ with a grid given by $\{r_j \in \mathbb{R}, j = 0, \ldots, N_1 + N_2\}$ where $h_j = r_j - r_{j-1}$, $r_0 = 0, r_{N_1} = R_i, r_{N_1+N_2} = R_o$. In time domain $[0, T]$ we introduce $\{t_n, n = 0, \ldots, M\}$ with $t_0 = 0, t_M = T$ and step-size Δt. Now, we describe the finite operators

$$\begin{aligned} &D_{cen}v(r_j) = \tfrac{v(r_{j+1})-v(r_{j-1})}{h_j+h_{j+1}}, \quad D_h v(r_{j+1/2}) = \tfrac{v(r_{j+1})-v(r_j)}{h_{j+1}}, \quad D_h^* v(r_j) = \tfrac{v(r_{j+1/2})-v(r_{j-1/2})}{h_{j+1/2}}, \\ &\hat{D_h} v\left(r_j\right) = \tfrac{2h_j+h_{j-1}}{h_j(h_j+h_{j-1})} v\left(r_j\right) - \tfrac{h_{j-1}+h_j}{h_j h_{j-1}} v\left(r_{j-1}\right) + \tfrac{h_j}{h_{j-1}(h_j+h_{j-1})} v\left(r_{j-2}\right), \\ &\bar{D_h} v\left(r_j\right) = \tfrac{-2h_{j+1}-h_{j+2}}{h_{j+1}(h_{j+1}+h_{j+2})} v\left(r_j\right) + \tfrac{h_{j+1}+h_{j+2}}{h_{j+1}h_{j+2}} v\left(r_{j+1}\right) - \tfrac{h_{j+1}}{h_{j+2}(h_{j+1}+h_{j+2})} v\left(r_{j+2}\right), \end{aligned} \tag{7}$$

where $h_{j+1/2} = \frac{h_j+h_{j+1}}{2}$.

Remark 3: Note that if the mesh is non-uniform, the centered operator D_{cen} is first order.

Remark 4: If $h_{j+1} \neq h_j$ we have that the local truncation error of $D_2^* v(r_j) = D_h^* \left(D_h v(r_j)\right)$ is bounded by

$$|T_{D_2^*}| \leq \frac{2}{3} h_{max} + \mathcal{O}(h_{max}^2). \tag{8}$$

By D_{-t} we denote the time backward finite difference operator. Let $C_{f,j}^n, C_{b,j}^n, C_{i,j}^n, D_{c,j}^n$ be the numerical approximations for the correspondent (r_j, t_n) and their respective finite difference equations

$$\begin{aligned} &D_{-t}C_{f,j}^{n+1} = \tfrac{D_f}{r_j^2} D_h^* \left(M_h(r_j^2) D_h C_{f,j}^n\right) - \tfrac{1}{r_j^2} D_{cen} C_{f,j}^n + S_{i,j}, \\ &D_{-t}C_{b,j}^{n+1} = \tfrac{D_b}{r_j^2} D_h^* \left(M_h(r_j^2) D_h C_{b,j}^n\right) - \tfrac{1}{r_j^2} D_{cen} C_{b,j}^n + k_a C_{f,j}^{n+1} - k_d C_{b,j}^n, \\ &D_{-t}C_{i,j}^{n+1} = V_{max}\left(\tfrac{C_{f,j}^{n+1}}{C_{f,j}^{n+1}+k_e\varphi} - \tfrac{C_{i,j}^n}{C_{i,j}^n+k_i}\right), \qquad D_{-t}D_{c,j}^{n+1} = \left(k_p - \tfrac{f_{max}C_{i,j}^{n+1}}{C_{i,j}^{n+1}+EC_{50}}\right) D_{c,j}^n - k_m \left(D_{c,j}^n\right)^2, \end{aligned} \tag{9}$$

where $M_h(r_j^2)$ is the average operator. We specify in what follows the discretization of the boundary conditions eq. (1) and eq. (4) using the discrete operators described in eq. (7).

At $r = R_o$ we consider

$$v_{R_o}^{n+1} C_{f,R_o}^{n+1} - D_{fn}\hat{D_h} C_{f,R_o}^{n+1} = 0, \qquad v_{R_o}^{n+1} C_{b,R_o}^{n+1} - D_b \hat{D_h} C_{b,R_o}^{n+1} = 0. \tag{10}$$

At $r = R_i$ we have

$$-D_{ft}\hat{D_h} C_{f,R_i}^{n+1} + D_{fn}\bar{D_h} C_{f,R_i}^{n+1} = 0, \qquad v_{R_i}^{n+1} C_{b,R_i}^{n+1} - D_b \bar{D_h} C_{b,R_i}^{n+1} = 0. \tag{11}$$

At $r = 0$ we consider

$$D_{cen} C_{f,r}^{n+1} = 0. \tag{12}$$

Finally, with the initial conditions

$$C_{f,j}^0 = 0, \quad C_{b,j}^0 = 0, \quad C_{i,j}^0 = 0, \quad D_{c,j}^0 = D_{co}, \quad j = 0, \ldots, N_1 + N_2, \tag{13}$$

we complete the finite-difference system eq. (9).

4 Numerical results

We illustrate some numerical simulations of our model eq. (9)- eq. (13) using the method described in the previous section. In the numerical implementation we use a time step $\Delta t = 10^{-5}$ and $h_j = 3.7 * 10^{-3}$ in $(0, R_i)$ and step size $h_j = 6.2 * 10^{-3}$ in (R_i, R_o). In the following, we find the figures for C_f, C_b, C_i, and D_c at different times T (in minutes), respectively.

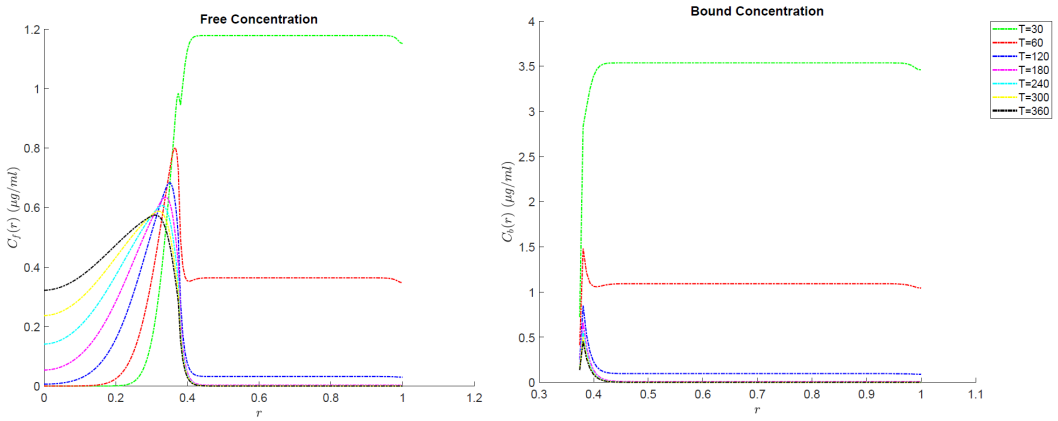

Figure 1. Free and Bound Doxorubicin Concentration in spatial domain respective with a dose $85600 \mu g/m^2$.

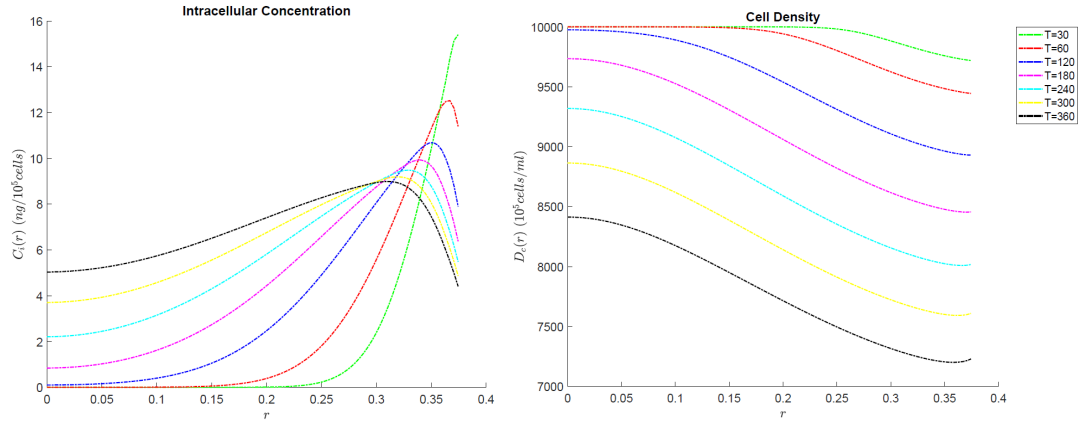

Figure 2. Intracellular Doxorubicin Concentration and, Density Cell in tumor domain with a dose $85600 \mu g/m^2$.

Fig. 1 and Fig. 2 show the radial distribution of concentrations and density at different times.

5 Conclusions

In Fig. 1 and Fig. 2, we note that for a sufficiently large time, the free concentration is less than the bound concentration. This behavior may be due to the exponential decay of the source term $C_v = D_d A e^{-\alpha t}$, where D_d is doxorubicin dose injected, A is the compartment parameter, and α is the compartment clearance rate. In addition, in comparison with the results in Zhan et al. [4], we observed that in our model, the concentrations are more retained in normal-tumor tissue for large times.

An increasing of doxorubicin dose leads to an higher level of drug concentration in all regions (normal and tumor tissue) and decay of tumor cell density, see Fig. 3

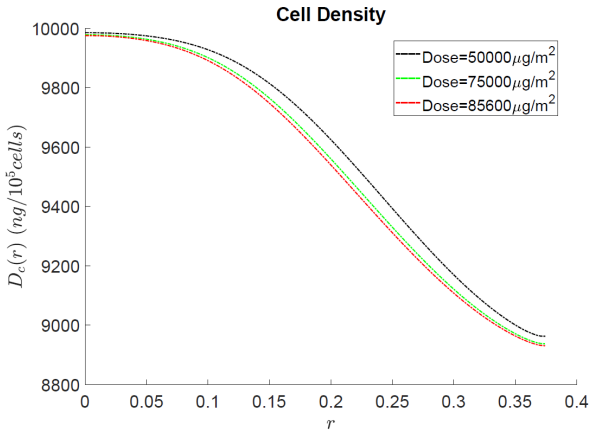

Figure 3. Tumor cell density at 120 minutes with different doses.

We observe in Fig. 1 that the following is satisfied for later times

$$C_b = \frac{k_a}{k_d} C_f \approx 3 C_f. \tag{14}$$

This justifies that the parabolic problem eq. (1) reaches the equilibrium already at $t = 30$ minutes when we have no source. In fact from $S_v + S_b = 0$ we can deduce directly the relation eq. (14).

[7]

Authorship statement. The authors hereby confirm that they are the sole liable persons responsible for the authorship of this work, and that all material that has been herein included as part of the present paper is either the property (and authorship) of the authors, or has the permission of the owners to be included here.

References

[1] L. T. Baxter and R. K. Jain. Transport of fluid and macromolecules in tumors. i. role of interstitial pressure and convection. *Microvascular research*, vol. 37, n. 1, pp. 77–104, 1989.

[2] S. Eikenberry. A tumor cord model for doxorubicin delivery and dose optimization in solid tumors. *Theoretical Biology and Medical Modelling*, vol. 6, n. 1, pp. 1–20, 2009.

[3] C. Liu, J. Krishnan, and X. Y. Xu. A systems-based mathematical modelling framework for investigating the effect of drugs on solid tumours. *Theoretical Biology and Medical Modelling*, vol. 8, n. 1, pp. 1–21, 2011.

[4] W. Zhan, W. Gedroyc, and X. Yun Xu. Mathematical modelling of drug transport and uptake in a realistic model of solid tumour. *Protein and peptide letters*, vol. 21, n. 11, pp. 1146–1156, 2014.

[5] A. W. El-Kareh and T. W. Secomb. A mathematical model for comparison of bolus injection, continuous infusion, and liposomal delivery of doxorubicin to tumor cells. *Neoplasia*, vol. 2, n. 4, pp. 325–338, 2000.

[6] J. S. Borges, J. A. Ferreira, G. Romanazzi, and E. Abreu. Drug release from viscoelastic polymeric matrices-a stable and supraconvergent fdm. *Computers & Mathematics with Applications*, vol. 99, pp. 257–269, 2021.

[7] R. E. Eliaz, S. Nir, C. Marty, and F. C. Szoka Jr. Determination and modeling of kinetics of cancer cell killing by doxorubicin and doxorubicin encapsulated in targeted liposomes. *Cancer research*, vol. 64, n. 2, pp. 711–718, 2004.